NASA PBL Convection and Extreme Weather White Paper Version 2 (10/1/2025)

Authored by the DSI PBL Convection and Extreme Weather Working Group

1. Summary

The planetary boundary layer (PBL) is where convective storms begin and where their greatest impacts are felt. Humidity, stability, and shear in the PBL are essential controls on the occurrence, structure, and intensity of deep, precipitating convection. However, the PBL varies widely in space and time, making it difficult to assess *why convection occurs where and when it does*. Current PBL observations are either made in-situ with high fidelity but poor spatial coverage, or from spaceborne sensors with good spatial coverage but insufficient space-time resolution for resolving many features associated with convective initiation and evolution. The *solution* is a space-based mission that can overcome existing resolution and retrieval limitations with advances in technology, particularly using sensors that can operate in cloudy and precipitating conditions associated with convective storms. Suborbital technology could complement and enhance the science benefits of space-based retrievals to observe processes at scales not possible from space.

NASA is well situated to become a leader in the development of this technology in the coming decade, including state-of-the-art advances in and synergistic use of hyperspectral microwave (MW) and infrared (IR), Global Navigation Satellite System (GNSS) radio occultation (RO), differential absorption radar (DAR) and lidar (DIAL), backscatter lidar (BSL), and multi-angle observing systems. Additionally, NASA Earth System Modeling (ESM) capabilities can rigorously quantify the value of a proposed satellite mission in terms of how it would improve our ability to understand and predict extreme weather and climate. Key applications of such a PBL mission are described and the satellite mission architecture is briefly discussed. A prototype Science and Applications Traceability Matrix (SATM) is also provided.

2. Motivation and Science Questions

The interaction between the PBL and convective storms is a key open topic in weather research, forecasting, and climate studies. The PBL thermodynamic structure (i.e., temperature and humidity profiles and PBL height) can determine whether convection occurs and can modulate the structure and severity of storms. Convective plumes grow out of the PBL, carrying with them PBL thermodynamic properties. Once convection initiates, PBL processes modulate the depth, intensity, and duration of convective systems. Downdrafts and heavy precipitation from deep convection then alter the PBL properties and composition, and delay the recovery of the PBL. Understanding these processes is critical to representing convection and extreme weather in a more realistic manner in weather and climate prediction models. These PBL-convection interactions motivate the three main scientific questions below and build upon the recommendation of the National Academies *2017-2027 Decadal Survey for Earth Science and Applications from Space* to improve the thermodynamic profiles and height characterization of the PBL to better understand the impact of the PBL on weather processes.

Q1. How do spatial and temporal variations in **pre-storm** PBL thermodynamics and height contribute to the initiation of convection and likelihood of severe weather?

Q2. What is the role of **near-storm** PBL thermodynamic and height variations in promoting or hindering the evolution of convection into deep, organized, or extreme events?

Q3: How do **post-storm** thermodynamic perturbations in the PBL impact PBL recovery and the timescale of initiation for subsequent convection?

3. Background on PBL Interactions with Convection and Extreme Weather

Our main interest is in PBL conditions associated with deep and/or precipitating convection (as occurs in isolated thunderstorms, organized mesoscale convective systems, and extratropical cyclones) and related phenomena (such as cold pools and the diurnal cycle of precipitation), because of their relevance to society. Extreme convective storm types include supercells, squall lines, tropical cyclones, and atmospheric rivers, while extreme weather impacts include hail, tornadoes, lightning, strong winds, flooding, and aviation turbulence and icing. Many of these impacts can occur in both regular and extreme convective storm types. The following grand challenges encompass longstanding obstacles in understanding and predicting convective storm evolution and can be addressed by a NASA PBL mission:

1. Determine the PBL processes most important in controlling the occurrence, depth, intensity, and organization of convective storms.
2. Understand and accurately model the complex interactions between convection and the PBL, especially in the model convective gray zone of roughly 200 m to 10 km horizontal grid resolution.

Three primary ingredients are required for the development of convection: lift, instability, and moisture (Doswell 1987, Johns and Doswell 1992, Doswell et al. 1996, Galarneau et al. 2023). While all three ingredients are important, this white paper focuses on the thermodynamic properties of the PBL (i.e., instability and moisture) as those are the main variables to be observed by the PBL mission, with wind considered an important ancillary variable. In terms of the three science questions in Section 2, the relevant PBL thermodynamic processes and temporal/spatial scales are highlighted below and in Figure 1.

Pre-storm: Presence or development of temperature and humidity gradients/boundaries and other spatial heterogeneities in the PBL that result in convective initiation. Moisture convergence can result in PBL deepening and reduces the likelihood of the dilution of air parcels as they ascend.

Near-storm: Temperature and humidity ingested into the storm updraft through storm inflow. The interaction of storms with thermodynamic boundaries can impact their severity, and the properties of cold pools that force new convective initiation.

Post-storm: PBL recovery following cooling due to diabatically cooled downdrafts determines the likelihood of additional convective initiation and the modulation of existing storms.

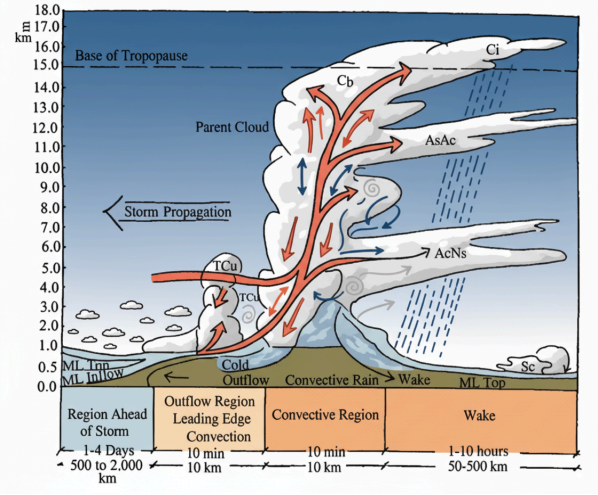

Figure 1. Schematic of pre-storm (1 day, 500 km), near-storm (10 min, 10 km), and post-storm (1-10 hours, 50-500 km) PBL and convection interactions. Adapted from Garstang and Fitzjarrald (1999).

PBL thermodynamics can vary greatly over small distances, with observed gradients in boundary layer water vapor mixing ratio of 1-4 g kg^{-1} across spatial scales < 10 km (Reinking et al. 1981, Weckwerth et al. 1996, Weckwerth 2000, Marquis et al. 2021). PBL thermodynamic variability influences the spatial distribution of important convective parameters such as CAPE and CIN. For example, the 3-km High-Resolution Rapid Refresh model has shown that horizontal heterogeneities in PBL temperature and humidity meaningfully perturb pre-storm CAPE in the southeastern US (Katona et al. 2016, Katona and Markowski 2021), while two near-simultaneous soundings from VORTEX2 separated by 35 km showed mixed-layer CAPE differences > 2000 J/kg (Klees et al. 2016).

The spatiotemporal variability of PBL thermodynamics maps strongly onto convective initiation location and timing. Crook (1996) showed that variations in PBL moisture as small as 1 g kg^{-1} and temperature as small as 1°C can determine convective initiation success or failure for modeled Colorado storms. Viscardi et al. (2025) showed that a reduction of just 4 mm in column water vapor below 1.5 km height can nearly suppress the formation of ice water in modeled convective clouds over the Amazon. In contrast, a similar effect in the free troposphere requires a much larger reduction in water vapor. Adams et al. (2017) used GNSS observations over the Amazon to show that PBL moisture convergence at horizontal scales < 50 km is important for the transition from shallow to deep convection. Over the ocean, Li and Carbone (2012) found that convective onset favors the edge of mesoscale warm oceanic patches with spatial scales of 10-50 km that likely change the adjacent PBL thermodynamics. Adding focused thermodynamic and wind profile observations in key regions before storm formation can result in better convective forecasts (Coniglio et al. 2019).

The PBL thermodynamic structure is strongly tied to the time of day and can vary rapidly. Daytime heating impacts PBL depth, especially over land, but the timing of convection can vary widely (Yang and Slingo 2001 and many other studies). Observations over the Amazon show that days with deep convection have moister-than-average conditions below 3 km early in the morning (Viscardi et al. 2024) and that the convergence of water vapor happens quickly, building up over about three hours before the transition to deep convection and reaching maximum speed within one hour of the event (Adams et al. 2017). A similarly fast increase in PBL moisture happens over the ocean during shallow convective growth (Bellenger et al. 2015). Atmospheric profiling over China showed three-hourly CAPE changes of up to 2000 J kg^{-1} and CIN of up to 400 J kg^{-1} associated with convective initiation (Pan et al., 2020).

Such variations in PBL thermodynamic characteristics have quantifiable impacts on organized severe convective storms and their associated hazards. Over land, 70% of supercell thunderstorm tornadoes were associated with low-level boundaries during VORTEX2 with tornadoes forming on the cool side of the boundaries in the region of greater low-level moisture (Markowski et al. 1998). Increased PBL stability due to nocturnal cooling results in a reduction in convective storm cold pool temperature deficits, which limits the lifting of air parcels by a storm's cold pool and can lead to a stagnation of supercells (Ziegler et al. 2010) and squall lines (Parker 2008). However, further cooling can lead to the development of a boundary layer bore that sustains squall lines overnight.

Large gradients in PBL temperature and humidity exist across coastlines and over mountains, with significant impacts on convective evolution. Thermally-driven boundary layer circulations near coasts lead to daytime convection over land (Kollias et al. 2025) and nighttime convection offshore (Bai et al. 2021, Fang and Du 2022). Cold pools associated with convective storms further interact with the PBL gradients, enhancing convective development (Lombardo and Kading 2018, Lombardo 2020). Terrain often triggers deep convection in the afternoon, and its off-terrain propagation and persistence strongly depends on local PBL properties (Geerts et al. 2017). The PBL over complex terrain also alters the behavior of propagating organized deep convection (Frame and Markowski 2006, Miglietta and Rotunno 2009), especially along mountainous coastlines (Wu and Lombardo 2021, 2023).

Many past studies have focused on PBL variations over land because of the lack of in-situ measurements over the ocean. The few measurements of PBL structure that exist are made over islands (e.g., the DOE ARM site in the Azores and the WFIP3 observations off the US East Coast), but islands

affect the PBL so are not representative of the open ocean. The marine PBL below tropical cyclones (TCs) has been measured mostly with dropsondes, which have excellent vertical resolution but lack horizontal space/time resolution. PBL humidity variations around tropical disturbances are consequential in modulating deep convection and TC genesis (Gao et al. 2019). In a composite sense, the TC boundary layer often exhibits an asymmetric structure of temperature, moisture, and height, that is organized by larger-scale environmental factors (e.g., 850-200 hPa wind shear) (Zhang et al. 2013). This asymmetry can impact the onset of TC genesis and intensification (Rappin and Nolan 2012). A developing eyewall often experiences dry air intrusions into the PBL from the environment or nearby inner-core convective cold pools, which hinders TC intensification (Tang and Emanuel 2012). The onset and rate of intensification depends on how effectively the PBL recovers from these intrusions and supports axisymmetrization of deep convection (Chen et al. 2021). TC rainband convection can generate cold pools that trigger newer convection of an incipient secondary eyewall. The evolution and distribution of PBL temperature and moisture can determine if and where a secondary eyewall forms, which impacts TC intensity, wind field size, and precipitation structure (Didlake et al. 2018, Yu et al. 2022).

Extratropical cyclones and atmospheric rivers (ARs) are other marine storms that are usually dominated by stratiform precipitation (Rabinowitz et al. 2019), but can contain embedded convection due to strong low-level convergence and instability (Cannon et al. 2020). Convection within ARs causes significant impacts when making landfall, with localized areas of intense rainfall that contribute greatly to total precipitation and flooding along the west coast of the US (Gershunov et al. 2017, Corringham et al. 2018). Furthermore, ARs can extend into the Arctic Ocean basin and play a crucial role in controlling sea ice variability, particularly during the ice growth season. However, understanding how convection develops within ARs and the role PBL processes play in their development remains a work in progress, particularly as convective schemes within weather models struggle to capture it (Luna-Niño et al., 2025). In high latitude marine cold air outbreaks (MCAOs), the advection of cold air over a progressively warmer ocean surface is associated with lightly precipitating shallow convection and a more broken cloud deck that causes large changes to reflected solar radiation. The co-evolution of MCAO PBL humidity and temperature structure is important for understanding how quickly and to what extent this cloud transition occurs (Tornow et al. 2023).

4. Space-Based Technology

4.1. Critical spaceborne technology for a PBL mission

The relationships between the PBL and convection detailed in Section 3 motivate the PBL measurement requirements listed in the Appendix, with emphasis placed on the necessary vertical and horizontal resolution to answer the three science questions in Section 2. Table 1 summarizes information on current and emerging technology capable of resolving PBL thermodynamic structure and height from space according to Teixeira et al. (2025) and information presented at community meetings as part of the NASA Decadal Survey Incubation PBL program. Active sensors like DAR and DIAL are currently assumed to fall outside the budgetary scope of a PBL space-borne mission, but technology advances are still being pursued for potential future flight opportunities. However, DIAL and DAR would provide valuable observations in suborbital campaigns (see Section 5.1). Emerging hyperspectral IR and MW technologies with finer horizontal and vertical resolution than currently available should be leveraged for a NASA mission focused on convection and extreme weather and the PBL. GNSS-RO provides fine vertical resolution in all-sky conditions, albeit with coarse horizontal resolution so would be best utilized in a data fusion framework with hyperspectral IR and MW observations. Additionally, BSL has been proposed to help constrain the PBL thermodynamic environment in the presence of clouds via data fusion with hyperspectral MW observations by identifying cloud top heights to constrain radiances. This data fusion capability can further be extended (beyond cloud top height identification) to DIAL in the future to utilize direct measurements of humidity as a constraint on IR and MW radiances.

Table 1. Critical sensors for a PBL convection and extreme weather space-based mission

Method	Orbit	PBL vertical x horizontal resolution		Conditions
		Current	*Emerging*	
Hyperspectral IR[1]	GEO LEO	1 km x 4-16 km 1 km x 2-14 km	500 m x 1 km	Clear sky, above clouds, broken clouds, thin clouds with cloud optical depth < 1
Hyperspectral MW[2]	LEO	2 km x 10-75 km	1 km x 10-20 km	All sky
GNSS-RO[3]	LEO-MEO	100 m x 100 km		All sky
Lidar[4]	LEO	PBL height (100 m x 1 km)		Clear sky, above clouds, broken clouds

[1]*Hyperspectral IR PoR*: MTG-S1/2, Himawari, GSX, AIRS, CrIS, IASI
[2]*Hyperspectral MW PoR*: NEON SMBA, Spire's HyMS, NASA HyMS/AURORA Pathfinder
[3]*GNSS-RO PoR*: Available GNSS-RO receivers provide thousands of thermodynamic profiles per day
[4]*Lidar PoR*: EarthCARE ATLID HSRL, ADM-AEOLUS, ASI-NASA LUCE

Hyperspectral IR: Infrared sensors can make retrievals in clear sky or mostly clear parts of the atmosphere, so are appropriate for observing small-scale PBL heterogeneities critical to convective initiation in pre-storm conditions. PBL retrievals can also be made in partially cloudy conditions near storms, with higher horizontal resolution observations minimizing cloud contamination when making retrievals in gaps between clouds. Emerging hyperspectral IR technologies may achieve a vertical resolution of 500 m with horizontal resolution of 1 km (Kurowski et al. 2023).

Hyperspectral MW: Microwave sensors can see through clouds and light rain, so are appropriate for observing PBL thermodynamic properties in all conditions (i.e., pre-, near-, and post-storm). NASA's AURORA Pathfinder mission (Gambini et al. 2024, Gambacorta et al. 2025) will improve vertical and horizontal resolution (i.e., to 1 km x 10 km) compared to the PoR. In addition, Gambacorta et al. (2023) showed that appropriate channel selection can improve lower and free tropospheric thermodynamic retrievals by up to 40% when compared against the Advanced Technology Microwave Sounder (ATMS).

GNSS-RO: Radio occultation provides high (100 m) vertical resolution thermodynamic retrievals in the PBL while resolving the diurnal cycle through its distributed network of spaceborne sensors (Nelson et al. 2021). Horizontal sensor resolution is limited to about 100 km by the nature of the technique; however, with more samples in a region, a tomography approach can improve the approximate horizontal resolution. GNSS-RO can be used in highly cloudy and precipitating environments like TCs (Vergados et al. 2013, Lasota et al. 2020, Nelson et al. 2025) and ARs (Haase et al. 2021, Cao et al. 2025, Rahimi and Foelsche 2025). It can also be used in joint retrievals with sounders (Wang et al. 2024) and added sensors in a close-formed constellation around the primary satellite (Leroy et al. 2020, Fitzgerald et al. 2021) could provide improved retrievals of PBL thermodynamic vertical structure. Polarimetric GNSS-RO (Padullés et al. 2016, Paz et al. 2024) utilizes horizontally and vertically polarized GNSS signals and the shapes of cloud and precipitation droplets to accumulate differential phase shift along the ray path, which can indicate the presence and effects of different hydrometeors.

Lidar: Spaceborne atmospheric lidars have employed either attenuated backscatter (i.e., BSL) or high spectral resolution techniques. Mature techniques like DIAL (yet to be implemented in space) measure profiles of water vapor in addition to profiles of attenuated backscatter (Barton-Grimley and Nehrir 2024). Any variant of spaceborne atmospheric lidar can estimate PBL height at < 100 m vertical and ~1-8 km (strong SNR dependence) horizontal resolution by identifying gradients in aerosol backscatter at the top

of the PBL (McGrath-Spangler et al. 2013, Palm et al. 2021). Utilization of lidar-derived clear air or cloud capped PBL height can serve as a constraint on IR and MW radiances with the potential to improve the thermodynamic retrievals from IR and MW sounders within the PBL (Kotsakis et al. 2023; Gambacorta et al. 2024, 2025). Utilization of humidity profiles from DIAL can directly constrain water vapor radiances for IR and MW to further improve PBL thermodynamic retrievals (Turner and Lohnert 2020).

4.2. The program of record (PoR)

The PoR encompasses sensors already in space or planned for launch by the early 2030s (Table 1). The PoR provides some PBL information, but current hyperspectral IR, hyperspectral MW, and RO instruments have coarse (~10-100 km) horizontal resolutions that will not resolve the most important spatial heterogeneities associated with convective processes. While some recently launched hyperspectral IR sensors have horizontal resolutions < 10 km, they target clear-sky conditions, which limits their use close to convective storms. Finally, all current hyperspectral IR and MW sensors in LEO are in sun-synchronous orbits and are limited in the times of day they sample, such that the full diurnal cycle is not observed. Hyperspectral IR is the only technology in Table 1 in GEO.

The Appendix lists ancillary geophysical variables associated with convection and wind that have known sources in the PoR. Visible, IR, and passive MW imagers (i.e., sensors with fewer channels emphasizing temporal and horizontal instead of vertical resolution and larger spatial coverage), lightning mappers, and spaceborne and ground radars will provide essential information on convective characteristics (such as storm height, area, intensity, and rainfall) necessary to link PBL properties to convection and extreme weather. PoR scatterometers, synthetic aperture radar, and passive MW radiometers will provide surface wind retrievals over the ocean to complement the thermodynamic retrievals from a PBL mission. In particular, the multi-agency Satellite Needs Working Group (SNWG) approved the Multi-Sensor Worldwide Ocean Winds (MWOW) solution in 2022 to provide observations of gridded near-surface winds every ~6 hours. Ground observations and reanalysis will be leveraged for low-level wind fields over land. An SNWG PBL product using GNSS-RO and PoR sounder data is also currently under development and the NOAA Products Validation System (NPROVS) provides satellite and sonde matched data across the globe.

4.3. Mission architecture

Most deep convection occurs in the tropics with additional enhancements over some extratropical land and storm track regions (Fig. 2, left panel). Deep convection initiates and evolves throughout the day, with an especially strong diurnal cycle over land (Figure 2, right panel), and has different diurnal timing over land and ocean (e..g, Yang and Slingo 2001). Thus, diurnally-resolved PBL measurements that can observe hourly variations (the time scale of the development of an individual convective cell) are essential to studying the interactions between the PBL and convection/extreme weather.

Diurnal sampling would most efficiently be addressed by an inclined orbit, which will not sample individual storm evolution but would allow statistical sampling of the diurnal cycle. TRMM and GPM effectively used this strategy to understand convective processes across the globe (e.g., Nesbitt and Zipser 2003). The PoR (especially from GEO) would provide context on storm evolution when individual event snapshots are sampled from the inclined orbit. Constellations of small satellites can further enhance diurnal sampling, such as with TROPICS and Tomorrow.io. Extending the inclination beyond 65° would significantly degrade diurnal sampling with little additional sampling of convection. Thus, the target inclination angle for a mission focusing on PBL and convection would be 50 to 65°. The need for diurnally-resolved PBL measurements could potentially be met with several sun-synchronous satellites with equatorial crossing times spaced out throughout the day, but the cost and need for co-located or closely-spaced (as in the A-Train configuration) hyperspectral IR and MW sensors makes this option more expensive than a single satellite with inclined orbit.

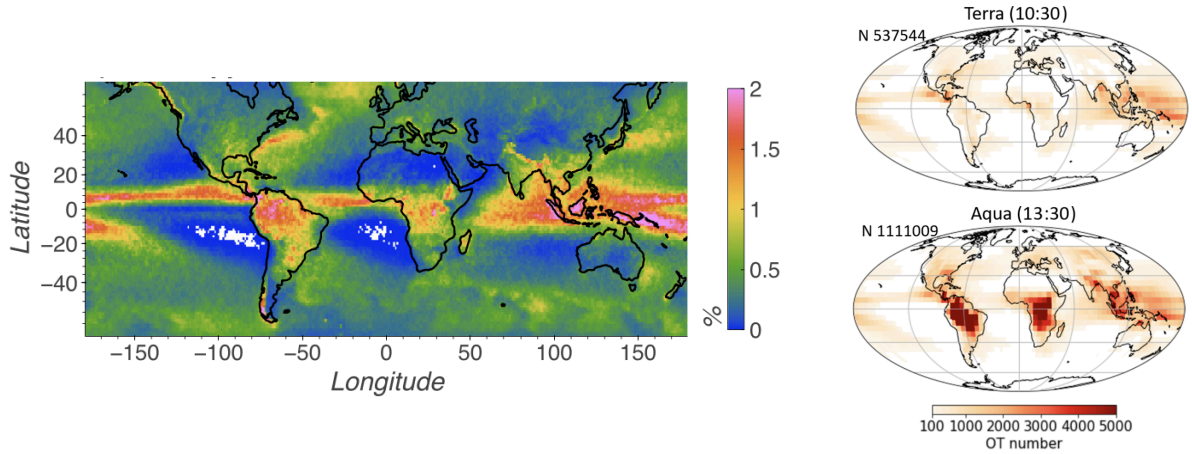

Figure 2. (left) Annual mean cold-topped convective area coverage from the GPM radar (Schumacher and Funk 2023). (right) Global distribution of overshooting convective cloud tops sampled from MODIS on Terra and Aqua during their 10:30 am and 1:30 pm LT overpasses, respectively (Hong et al. 2023).

In addition to the above sensor and architecture discussion, two additional strategies may be considered for investigating PBL and convection interactions: multi-angle observations and delta-t sampling. Multi-angle measurements provide 3D atmospheric volumes and dynamics in the PBL at high spatial resolution. Tomographic methods can retrieve volumetric cloud and aerosol microphysics (Levis et al. 2015, 2020, 2021; Loveridge et al. 2023ab) as well as 3D temperature and humidity fields (Forster et al. 2025), achieving < 100 m resolution in the vertical and horizontal for VIS/SWIR imagery. 3D macrophysical properties and motion vectors are accessible through stereoscopic techniques (Zhao and Di Girolamo 2007; Dey et al. 2008, De Vera et al. 2024; Di Girolamo et al. 2025). The tomographic techniques discussed in Forster et al. (2025) and used for GNSS-RO could be used for different combinations of sensors and with architectures ranging from single platforms to constellations and LEO-GEO combinations, potentially unlocking major improvements in 3D retrievals in the PBL.

Delta-t sampling is time-separated "snapshots", e.g. from two satellites separated by 10 min, that can be used to measure PBL thermodynamics and their temporal evolution. These snapshots could also be used to retrieve vertical profiles of horizontal winds (Ouyed et al. 2023) and permit computation of horizontal divergence (Zeng et al. 2024). Multi-angle VIS/SWIR imager 3D cloud retrievals can provide fine-precision wind fields (Loveridge and Di Girolamo 2025).

5. Suborbital Observations, Models, and Data Fusion

5.1. PBL suborbital component

There is a strong need for a suborbital component of the PBL mission. Motivations include:

1. Calibration and validation of spaceborne sensor observations with airborne sounders and in-situ observations.
2. Development and assessment of spaceborne sensor algorithms and PBL retrievals.
3. Observation of PBL processes and ancillary variables not viewable by the mission architecture or from the PoR (e.g., time evolution, winds, cloud microphysics and dynamics, aerosols).
4. Technology development for future spaceborne missions.

Table 2 lists sensors (i.e., DIAL, DAR, and Doppler wind lidar) that can provide exceptional vertical and horizontal resolution characterization of PBL properties and that would be heavily utilized in the

suborbital component of the mission. Airborne versions of the sensors in Table 1 (i.e., hyperspectral IR, hyperspectral MW, GNSS-RO, and BSL) already exist and would also be heavily utilized. The suborbital component should commence before launch of the satellite mission, providing a bridge to early adoption of the spaceborne observations and products (i.e., PBL-now).

Table 2. Critical sensors for PBL convection and extreme weather suborbital component in addition to airborne versions of sensors in Table 1

Method	**PBL vertical x horizontal resolution**		**Conditions**
	Current	*Emerging*	
Differential absorption lidar (DIAL)	300 m x 6 km	100 m x 1 km	Clear sky and into cloud within lidar extinction limit
Differential absorption radar (DAR)	300 m x 10 km	200 m x 5 km	Cloud/moderate rain
Doppler wind lidar	66 m x 2 km	30 m x 1 km	Clear sky and into cloud within lidar extinction limit

Differential absorption lidar (DIAL): Airborne DIAL is capable of directly measuring water vapor with high precision, accuracy, and resolution throughout the troposphere and lower stratosphere by transmitting at multiple nearby wavelengths distributed along a near-IR water vapor absorption feature. The High-Altitude-Lidar Observatory (HALO) is the only US airborne water vapor DIAL and High Spectral Resolution Lidar. It supports NASA airborne science campaigns and serves as a technology testbed to mature and demonstrate DIAL technologies for future missions (Carroll et al. 2022).

Differential absorption radar (DAR): Airborne DAR is the microwave analogue of DIAL. By transmitting at multiple frequencies in the wings of the 183 GHz water vapor absorption line, DAR is able to derive vertical profiles of water vapor concentration in cloudy and moderately precipitating conditions. Typical resolutions for DAR measurements are 300 m x 10 km, but accuracy and resolution can be traded in post-processing depending on the application. DAR can also provide high-resolution measurement of the column-integrated water vapor in all but the most heavily precipitating conditions. The Vapor In-cloud Profiling Radar (VIPR) is a DAR technology demonstration project that has recently transitioned to operations in support of the NASA airborne science program (Millán et al. 2024).

Doppler wind lidar: Airborne coherent-detection Doppler wind lidars (CDWL) such as the NASA LaRC Airborne Wind Profiler (AWP) measure atmospheric backscatter from clear sky aerosol and clouds and Doppler shifts caused by aerosol/cloud motions. AWP measures at multiple lines of sight, enabling retrieval of wind vector profiles. CDWLs are well suited for PBL measurement because the PBL is often aerosol-rich. AWP also measures the vertical wind component via lidar pulses directed at nadir. AWP serves as a testbed to mature and demonstrate wind lidar technologies for future missions.

In addition to aircraft versions of the sensors in Table 1, DIAL, DAR, and Doppler wind lidar would be deployed on aircraft in a set of field campaigns or transects that are representative of a range of deep convective environments (e.g., dry/continental, moist/continental, moist/oceanic). These campaigns or transects would be synergistic with the PBL cloud and/or surface-interaction groups. Emphasis would be placed in studying PBL-convective interactions at a process level (e.g., transect sampling would require times to stop and observe convective evolution). High temporal sampling of pre, near-, and post-storm conditions would be made to determine what intermittent satellite sampling can not observe. The Westcoast and Heartland Hyperspectral Microwave Sensor Intensive experiment (WH2yMSIE) provided

an excellent data set of co-registered passive and active sensors, serving as a valuable opportunity to test novel technologies (e.g., CoSMIR-H and MBARS) and data fusion techniques, and providing a roadmap for suborbital field deployments. Very high resolution modeling (e.g., large-eddy simulations) could also be leveraged to better characterize the 3D PBL variations that can not be observed. The DOE LASSO program is applying this concept to deep convective case studies over Argentina.

5.2. Suborbital PoR

Similar to the space-based PoR discussion in Section 4.2, any suborbital effort would leverage and build upon existing non space-based PBL resources, including ground sites and facilities run by other groups, past field campaigns, and ongoing community efforts.

Ground sites/facilities: DOE and NOAA have deployed long-term PBL measurements at fixed and mobile sites around the globe (e.g., through the DOE ARM program) and facilities capable of measuring PBL properties are available for request through programs such as NSF MAPnet and UAH CIF. State mesonets like New York State Mesonet consisting of surface, profiler and flux networks (Shrestha et al. 2021) could also be utilized along with networks like the GEWEX Land-Atmosphere Feedback Observatory (GLAFO, Wulfmeyer et al. 2021), which provides comprehensive measurements of land surface processes and PBL processes (including turbulent fluxes) over different regions.

Past field campaigns: The following field campaigns have captured observations of the PBL and convection and represent significant community interest and a continuing need to better understand the PBL and its relationship to convection and extreme weather: IHOP (2002), GRIP (2010), MC3E (2011), SNPP (2013), IPHEx (2014), PECAN (2015), GOES-PLT (2017), CPEX (2017), CPEX-AW (2021), CPEX-CV (2022), TRACER/TRACER-AQ/ESCAPE (2022), ALOFT (2023), WH2YMSIE (2024), ICECHIP (2025), Enlighten (planned 2028).

Community efforts: The Global Precipitation Experiment (GPEX) is a decade-long Lighthouse Activity of the World Climate Research Programme (WCRP) (Zeng et al. 2025). Its central phase is the coordinated global field campaigns focusing on different storm types (ARs, mesoscale convective systems, monsoons, and TCs, among others) over different regions and seasons. It is seeking “anchor projects” for each storm type, and the PBL mission-related field campaigns could coordinate with GPEX activities, including possibly becoming an anchor project.

5.3. Modeling and data fusion

Modeling: A future PBL mission should provide data of value to modeling and forecasting applications. This value can be quantified in terms of short-term forecast skill improvements, e.g., as provided by NASA's GEOS model. Here, data assimilation methods combine observations with the model to correct, constrain, and quantify uncertainty in the forecast. Value can also be quantified in terms of long-term climate (approaching centennial) predictions, e.g., as provided by NASA's ModelE ESM. Here, errors in the statistics of Earth’s climate properties are primarily the result of misspecified or uncertain process parameterizations (e.g., how clouds are represented in models), rather than the initial state of the atmosphere. Therefore, observations are used to refine model representation of physical processes through the process of parameter estimation or by using observations to develop new parameterizations.

In both cases, we emphasize the need to perform Observing System Simulation Experiments (OSSE) to quantify the value of proposed observations for data assimilation or parameter estimation. The former methodology is well-established (Zeng et al. 2020). The latter is a new capability, leveraging recent work that uses artificial intelligence (AI) and Bayesian inference to autocalibrate model parameters with uncertainty quantification (Elsaesser et al. 2025). This methodology allows for a "Climate OSSE"

(Fridlind et al. 2025) wherein the value of a proposed observation is quantified in terms of knowledge gained on model parameters, as well as in terms of reduced uncertainty in projection of convective feedbacks and convection-relevant climatic impact-drivers (Ruane et al. 2022).

We note that data assimilation systems can combine a wide range of observations cohesively with model physics to provide better global PBL structure analysis for both model initialization as well as better scientific understanding of convective processes. For example, the assimilation of high-temporal resolution radar-derived PBL height statistically improves rainfall forecasts for a torrential rainfall and flashflood event through a better representation of lower-tropospheric moisture (Zhang et al. 2025). The assimilation of the vertical profile of water vapor mixing ratio from a surface-based Raman lidar and DIAL during PECAN improved both the PBL moisture and wind fields and led to improved forecast of precipitation associated with a mesoscale convection system (Carroll et al. 2021).

Parameterization development and improvement via, e.g., parameter estimation, is capable of improving not only ESMs, but also NWP models, which also suffer from errors due to parameterization uncertainties. Coniglio et al. (2013) evaluated five WRF PBL parameterization schemes with sounding observations. However, Olson et al. (2019) had more success evaluating the MYNN-EDMF PBL and shallow cloud scheme using higher resolution Wind Forecast Improvement Project observations.

AI and data fusion: The rapidly evolving field of AI can be used for improved forecasting and retrievals. Explainable AI can be further leveraged for better physical understanding of PBL and convection interactions. WOFS-Cast (Flora and Potvin 2025) and HRRR-Cast (in review) are two recent regional AI-driven weather prediction models, among many others. However, none of them have been trained on PBL properties. Passive-active data fusion using AI has been demonstrated to be key in improving information content in PBL thermodynamics retrievals. Turner and Lohnert (2021) and Gambacorta et al. (2025) have demonstrated this retrieval approach using passive MW and lidar data. These active/passive techniques will fill the information gap of single sensors. A data fusion approach will be essential to achieve the desired measurement requirements listed in the Appendix, since no single instrument meets all of the requirements.

6. Societal Needs and Applications

The fine spatiotemporal scales at which convection forms and evolves, together with potentially severe societal impacts, present unique challenges for stakeholders which improved PBL observations can address. These stakeholders include government (e.g., the National Oceanic and Atmospheric Administration [NOAA], Federal Emergency Management Agency [FEMA], US Forest Service [USFS], US Department of Agriculture [USDA], Department of Defense [DOD]), state and local emergency management, and private-sector (e.g., insurance, commodities, airlines, agribusiness, and energy) interests.

NASA's Earth Science to Action strategy enables the translation of basic scientific research and technical capabilities into products that provide actionable information for stakeholders. Translating PBL science to Earth Action and applications for societal benefit requires community collaboration across science and stakeholders to identify needs and co-develop solutions that lead to impact on decision-making. Engaging advanced users and improving models is a key enabling capability for PBL applications. Improving models and use of AI/ML to assimilate PBL observations enables the co-development of value-added products and model outputs for specific stakeholders and their decisions. Furthermore, novice stakeholders benefit from development of decision-ready formats and visualizations that are interpretable for their application (e.g., insurance, energy, transportation). This value chain from models to value-added solutions to decision-ready visualizations will lead to increased uptake of PBL observations by stakeholders, adoption for decision-making, and promotion of Earth Information as a National Asset. This strategy will be executed through established research-to-applications organizations such as NASA's Short-Term Prediction Research and Transition (SPoRT) Center to work with

stakeholders to identify their needs and address them using the new technological, research, and modeling capabilities detailed here. Some initially identified needs related to PBL convection include:

Forecasting and nowcasting convective initiation

Observing and modeling convection initiation requires observing platforms that can resolve and accurately predict PBL heterogeneities. These improved observational capabilities should also enable the development of better-refined convective indices which will assist with nowcasting convective initiation, improving severe weather warning lead-time, and aviation flight planning.

Understanding the contribution of convection to extreme flooding events

Most extreme flooding events are convectively driven and their duration and intensity often depend on PBL processes that are difficult to observe and model. Better understanding mesoscale convective systems and ARs that lead to flood events will improve forecasts and tools developed by public- and private- sector stakeholders to alert the public. This will enable improved response to extreme precipitation events by state and local emergency authorities and contribute to improving transportation and logistics decisions including supply chain management and interruptions.

Characterizing the risk of hail, tornado, and severe wind storms

Large hail, tornadoes, and severe wind storms can significantly affect crop yields and also inflict millions of dollars in insurable damage to structures and vehicles. Better characterizing the risk of these convectively driven events will help the commodities and (re)insurance industries to better anticipate risk.

Understanding tropical cyclone boundary-layer evolution

Boundary-layer processes play a critical role in TC intensification. A dearth of PBL observations has contributed to forecasting uncertainty – especially in rapid intensification – which is a significant threat to coastal communities that remains difficult to forecast. Improved modeling and forecasting will benefit federal, state, and local mitigation and response to coastal threats including flooding, high winds, and storm surge.

Lightning and wildland fires

It remains difficult to know when and where lightning will strike and which lightning strikes will ignite wildland fires. Better observations of PBL structure, together with lightning observations from the program of record, will advance understanding of lightning-initiated wildfire and the risks they pose to communities and stakeholders. This will improve wildfire risk mitigation by federal, state, local agencies and inform decisions and policies of power companies.

Radio frequency propagation and aerosol optical extinction

Low-level convective outflow can create stable layers in the boundary layer that facilitate ducting of electromagnetic waves. It can also produce aerosols that affect optical extinction in the boundary layer. Both these phenomena are of interest to DOD, as they can affect communications and weapons and defense systems- improving DOD decisions on safety, movement, and scenario planning.

Appendix: Simplified Science and Applications Traceability Matrix (SATM)

Geophysical Variables & Measurement Requirements	Potential Measurement Technologies
• Spatial distributions of T and q in clear and cloudy conditions Vertical res: 250 m - 500 m Horizontal res: 1 km (Q1), 5 km (Q2+Q3) Uncertainty: 1 K, 1g/m^{-3} • PBL height Horizontal res: 1 km (Q1), 5 km (Q2+Q3) Uncertainty: 200 m • Temporal sampling Diurnally resolved: - Multiple times per day at same location or statistical sampling of diurnal cycle	• Clear and partial cloudy (with COD < 1) - IR sounder - Shortwave multi-angle - Lidar (DIAL, BSL) • Clear and cloudy conditions - MW sounder - GNSS-RO - Radar (DAR) • Temporal sampling approaches - LEO inclined orbit (IR + MW sounders, lidar) - GEO (IR sounder) - Cubesat constellation (delta-t) - Suborbital (DIAL, DAR, Doppler lidar)
• Ancillary geophysical variables with known sources in PoR Convection: - Convective cloud top T and area - Rainfall - Lightning - Hail, tornadoes - Vertical motion Winds: - Surface winds - Profiles of horizontal wind - Vertical motion in PBL	• PoR sources for ancillary variables Convection data: - GEO (VIS, IR, and lightning) - LEO (IR, passive and active MW) - Ground radars Wind data: - LEO (Scatterometers, SAR, passive and active MW) - Ground stations, mesonets, soundings

References

Adams, D. K., H. M. J. Barbosa, and K. P. G. D. L. Ríos, 2017: A Spatiotemporal Water Vapor–Deep Convection Correlation Metric Derived from the Amazon Dense GNSS Meteorological Network. Monthly Weather Review, 145, 279–288, https://doi.org/10.1175/MWR-D-16-0140.1.

Bai, H., G. Deranadyan, C. Schumacher, A. Funk, C. E. Epifanio, A. Ali, Endarwin, F. Radjab, R. Adriyanto, N. Nurhayati, Y. Nugraha, and A. Fauziah, 2021: Formation of nocturnal offshore rainfall near the west coast of Sumatra: Land breeze or gravity wave? Monthly Weather Review, 149, 715-731, doi:10.1175/MWR-D-20-0179.1

Barton-Grimley, R. A., and A. R. Nehrir, 2024: Sensitivity analysis of space-based water vapor differential absorption lidar at 823 nm. Front. Remote Sens., 5, https://doi.org/10.3389/frsen.2024.1404877.

Bellenger, H., K. Yoneyama, M. Katsumata, T. Nishizawa, K. Yasunaga, and R. Shirooka, 2015: Observation of Moisture Tendencies Related to Shallow Convection. Journal of the Atmospheric Sciences, 72, 641–659, https://doi.org/10.1175/JAS-D-14-0042.1.

Cannon, F., and Coauthors, 2020: Observations and Predictability of a High-Impact Narrow Cold-Frontal Rainband over Southern California on 2 February 2019. Weather and Forecasting, 35, 2083–2097, https://doi.org/10.1175/WAF-D-20-0012.1.

Cao, B., J. S. Haase, M. J. Murphy Jr., and A. M. Wilson, 2025: Observing atmospheric rivers using multi-GNSS airborne radio occultation: system description and data evaluation. Atmospheric Measurement Techniques, 18, 3361–3392, https://doi.org/10.5194/amt-18-3361-2025.

Carroll, B. J., B. B. Demoz, D. D. Turner, and R. Delgado, 2021: Lidar Observations of a Mesoscale Moisture Transport Event Impacting Convection and Comparison to Rapid Refresh Model Analysis. Monthly Weather Review, 149, 463–477, https://doi.org/10.1175/MWR-D-20-0151.1.

——, A. R. Nehrir, S. A. Kooi, J. E. Collins, R. A. Barton-Grimley, A. Notari, D. B. Harper, and J. Lee, 2022: Differential absorption lidar measurements of water vapor by the High Altitude Lidar Observatory (HALO): Retrieval framework and first results. Atmospheric Measurement Techniques, 15, 605–626, https://doi.org/10.5194/amt-15-605-2022.

Chen, X., J.-F. Gu, J. A. Zhang, F. D. Marks, R. F. Rogers, and J. J. Cione, 2021: Boundary Layer Recovery and Precipitation Symmetrization Preceding Rapid Intensification of Tropical Cyclones under Shear. Journal of the Atmospheric Sciences, 78, 1523–1544, https://doi.org/10.1175/JAS-D-20-0252.1.

Coniglio, M. C., J. Correia, P. T. Marsh, and F. Kong, 2013: Verification of Convection-Allowing WRF Model Forecasts of the Planetary Boundary Layer Using Sounding Observations. Weather and Forecasting, 28, 842–862, https://doi.org/10.1175/WAF-D-12-00103.1.

——, G. S. Romine, D. D. Turner, and R. D. Torn, 2019: Impacts of Targeted AERI and Doppler Lidar Wind Retrievals on Short-Term Forecasts of the Initiation and Early Evolution of Thunderstorms. Monthly Weather Review, 147, 1149–1170, https://doi.org/10.1175/MWR-D-18-0351.1.

Corringham, T. W., F. M. Ralph, A. Gershunov, D. R. Cayan, and C. A. Talbot, 2019: Atmospheric rivers drive flood damages in the western United States. Science Advances, 5, eaax4631, https://doi.org/10.1126/sciadv.aax4631.

Crook, N. A., 1996: Sensitivity of Moist Convection Forced by Boundary Layer Processes to Low-Level Thermodynamic Fields. Monthly Weather Review, 124, 1767–1785, https://doi.org/10.1175/1520-0493(1996)124%253C1767:SOMCFB%253E2.0.CO;2.

Dey, S., L. Di Girolamo, and G. Zhao, 2008: Scale effect on statistics of the macrophysical properties of trade wind cumuli over the tropical western Atlantic during RICO. Journal of Geophysical Research: Atmospheres, 113, https://doi.org/10.1029/2008JD010295.

Di Girolamo, L., G. Zhao, G. Zhang, Z. Wang, J. Loveridge, and A. Mitra, 2025: Decadal changes in atmospheric circulation detected in cloud motion vectors. Nature, 643, 983–987, https://doi.org/10.1038/s41586-025-09242-1.

Didlake, A. C., P. D. Reasor, R. F. Rogers, and W.-C. Lee, 2018: Dynamics of the Transition from Spiral Rainbands to a Secondary Eyewall in Hurricane Earl (2010). Journal of the Atmospheric Sciences, 75, 2909–2929, https://doi.org/10.1175/JAS-D-17-0348.1.

Doswell, C. A., 1987: The Distinction between Large-Scale and Mesoscale Contribution to Severe Convection: A Case Study Example. Weather and Forecasting, 2, 3–16, https://doi.org/10.1175/1520-0434(1987)002%253C0003:TDBLSA%253E2.0.CO;2.

——, H. E. Brooks, and R. A. Maddox, 1996: Flash Flood Forecasting: An Ingredients-Based Methodology. Weather and Forecasting, 11, 560–581, https://doi.org/10.1175/1520-0434(1996)011%253C0560:FFFAIB%253E2.0.CO;2.

Elsaesser, G. S., and Coauthors, 2025: Using Machine Learning to Generate a GISS ModelE Calibrated Physics Ensemble (CPE). Journal of Advances in Modeling Earth Systems, 17, e2024MS004713, https://doi.org/10.1029/2024MS004713.

Fang, J., and Y. Du, 2022: A global survey of diurnal offshore propagation of rainfall. Nat Commun, 13, 7437, https://doi.org/10.1038/s41467-022-34842-0.

Fitzgerald, R., L. Halperin, S. Leroy, A. Gagnon, K. Cahoy, and J. Clark, 2021: Analyzing Constellation Performance for the Radio Occultation Tomography of Internal Gravity Waves. IEEE Journal of Selected Topics in Applied Earth Observations and Remote Sensing, 14, 7225–7236, https://doi.org/10.1109/JSTARS.2021.3080984.

Flora, M. L., and C. Potvin, 2025: WoFSCast: A Machine Learning Model for Predicting Thunderstorms at Watch-to-Warning Scales. Geophysical Research Letters, 52, e2024GL112383, https://doi.org/10.1029/2024GL112383.

Forster, L., 2025: Scientific applications of multi-angle measurements to reconstruct Earth's atmosphere through tomography. Bulletin of the American Meteorological Society, In Review.

Frame, J., and P. Markowski, 2006: The Interaction of Simulated Squall Lines with Idealized Mountain Ridges. Monthly Weather Review, 134, 1919–1941, https://doi.org/10.1175/MWR3157.1.

Fridlind, A. M., and Coauthors, 2025: Towards a Climate OSSE Framework for Satellite Mission Design, https://doi.org/10.48550/arXiv.2509.00211.

Galarneau Jr., T. J., X. Zeng, R. D. Dixon, A. Ouyed, H. Su, and W. Cui, 2023: Tropical mesoscale convective system formation environments. Atmospheric Science Letters, 24, e1152, https://doi.org/10.1002/asl.1152.

Gambacorta, A., and Coauthors, 2023: Advancing Earth's Planetary Boundary Layer Sounding from Space Using Hyperspectral Microwave Measurements. IGARSS 2023 - 2023 IEEE International Geoscience and Remote Sensing Symposium, IGARSS 2023 - 2023 IEEE International Geoscience and Remote Sensing Symposium, 1321–1324, https://doi.org/10.1109/IGARSS52108.2023.10282918.

——, and Coauthors, 2024: The West-Coast Hyperspectral Microwave Sensor Intensive Experiment (WHYMSIE). IGARSS 2024 - 2024 IEEE International Geoscience and Remote Sensing Symposium, 1430–1432, https://doi.org/10.1109/IGARSS53475.2024.10641560.

——, and Coauthors, 2025: Improved Planetary Boundary Layer Sounding Using Hyperspectral Microwave and Backscatter Lidar Data Fusion, IEEE Transactions in Geophysics and Remote Sensing, Accepted.

Gambini, F., R. Moreira, D. Robles, A. Gambacorta, and M. Stephen, 2024: An Ultra-Compact, Narrow-Bandwidth, and High-Density Channel Photonic Integrated Channelizer Based on Serial Arrayed Waveguide Grating Architecture. Journal of Lightwave Technology, 42, 2908–2916, https://doi.org/10.1109/JLT.2024.3349932.

Gao, S., S. Jia, Y. Wan, T. Li, S. Zhai, and X. Shen, 2019: The Role of Latent Heat Flux in Tropical Cyclogenesis over the Western North Pacific: Comparison of Developing versus Non-Developing Disturbances. Journal of Marine Science and Engineering, 7, 28, https://doi.org/10.3390/jmse7020028.

Garstang, M., and D. R. Fitzjarrald, 1999: Observations of Surface to Atmosphere Interactions in the Tropics. Oxford University Press 422pp.

Geerts, B., and Coauthors, 2017: The 2015 Plains Elevated Convection at Night Field Project. Bulletin of the American Meteorological Society, 98, 767–786, https://doi.org/10.1175/BAMS-D-15-00257.1.

Gershunov, A., T. Shulgina, F. M. Ralph, D. A. Lavers, and J. J. Rutz, 2017: Assessing the climate-scale variability of atmospheric rivers affecting western North America. Geophysical Research Letters, 44, 7900–7908, https://doi.org/10.1002/2017GL074175.

Haase, J. S., M. J. Murphy, B. Cao, F. M. Ralph, M. Zheng, and L. Delle Monache, 2021: Multi-GNSS Airborne Radio Occultation Observations as a Complement to Dropsondes in Atmospheric River Reconnaissance. Journal of Geophysical Research: Atmospheres, 126, e2021JD034865, https://doi.org/10.1029/2021JD034865.

Hong, Y., S. W. Nesbitt, R. J. Trapp, and L. Di Girolamo, 2023: Near-global distributions of overshooting tops derived from Terra and Aqua MODIS observations. Atmospheric Measurement Techniques, 16, 1391–1406, https://doi.org/10.5194/amt-16-1391-2023.

Johns, R. H., and C. A. Doswell, 1992: Severe Local Storms Forecasting. Weather and Forecasting, 7, 588–612, https://doi.org/10.1175/1520-0434(1992)007%253C0588:SLSF%253E2.0.CO;2.

Katona, B., and P. Markowski, 2021: Assessing the Influence of Complex Terrain on Severe Convective Environments in Northeastern Alabama. Weather and Forecasting, 36, 1003–1029, https://doi.org/10.1175/WAF-D-20-0136.1.

——, ——, C. Alexander, and S. Benjamin, 2016: The Influence of Topography on Convective Storm Environments in the Eastern United States as Deduced from the HRRR. Weather and Forecasting, 31, 1481–1490, https://doi.org/10.1175/WAF-D-16-0038.1.

Klees, A. M., Y. P. Richardson, P. M. Markowski, C. Weiss, J. M. Wurman, and K. K. Kosiba, 2016: Comparison of the Tornadic and Nontornadic Supercells Intercepted by VORTEX2 on 10 June 2010. Monthly Weather Review, 144, 3201–3231, https://doi.org/10.1175/MWR-D-15-0345.1.

Kollias, P., and Coauthors, 2025: Experiment of Sea Breeze Convection, Aerosols, Precipitation, and Environment (ESCAPE). Bulletin of the American Meteorological Society, 106, E310–E332, https://doi.org/10.1175/BAMS-D-23-0014.1.

Kotsakis, A., and Coauthors, 2023: Hyperspectral Microwave Measurement Demonstrations of Improved Thermodynamic Sounding from Space. IGARSS 2023 - 2023 IEEE International Geoscience and Remote Sensing Symposium, IGARSS 2023 - 2023 IEEE International Geoscience and Remote Sensing Symposium, 1448–1449, https://doi.org/10.1109/IGARSS52108.2023.10282289.

Kurowski, M. J., and Coauthors, 2023: Synthetic Observations of the Planetary Boundary Layer from Space: A Retrieval Observing System Simulation Experiment Framework. Bulletin of the American Meteorological Society, 104, E1999–E2022, https://doi.org/10.1175/BAMS-D-22-0129.1.

Lasota, E., A. K. Steiner, G. Kirchengast, and R. Biondi, 2020: Tropical cyclones vertical structure from GNSS radio occultation: an archive covering the period 2001–2018. Earth System Science Data, 12, 2679–2693, https://doi.org/10.5194/essd-12-2679-2020.

Leroy, S., R. Fitzgerald, K. Cahoy, J. Abel, and J. Clark, 2020: Orbital Maintenance of a Constellation of CubeSats for Internal Gravity Wave Tomography. IEEE Journal of Selected Topics in Applied Earth Observations and Remote Sensing, 13, 307–317, https://doi.org/10.1109/JSTARS.2019.2961084.

Levis, A., Y. Y. Schechner, A. Aides, and A. B. Davis, 2015: Airborne Three-Dimensional Cloud Tomography. 2015 IEEE International Conference on Computer Vision (ICCV), 2015 IEEE International Conference on Computer Vision (ICCV), 3379–3387, https://doi.org/10.1109/ICCV.2015.386.

——, ——, A. B. Davis, and J. Loveridge, 2020: Multi-View Polarimetric Scattering Cloud Tomography and Retrieval of Droplet Size. Remote Sensing, 12, 2831, https://doi.org/10.3390/rs12172831.

——, A. B. Davis, J. R. Loveridge, and Y. Y. Schechner, 2021: 3D cloud tomography and droplet size retrieval from multi-angle polarimetric imaging of scattered sunlight from above. Polarization Science and Remote Sensing X, Vol. 11833 of, Polarization Science and Remote Sensing X, SPIE, 31–45, https://doi.org/10.1117/12.2593369.

Li, Y., and R. E. Carbone, 2012: Excitation of Rainfall over the Tropical Western Pacific. Journal of the Atmospheric Sciences, 69, 2983–2994, https://doi.org/10.1175/JAS-D-11-0245.1.

Lombardo, K., 2020: Squall Line Response to Coastal Mid-Atlantic Thermodynamic Heterogeneities. Journal of the Atmospheric Sciences, 77, 4143–4170, https://doi.org/10.1175/JAS-D-20-0044.1.

——, and T. Kading, 2018: The Behavior of Squall Lines in Horizontally Heterogeneous Coastal Environments. Journal of the Atmospheric Sciences, 75, 1243–1269, https://doi.org/10.1175/JAS-D-17-0248.1.

Loveridge, J., and L. Di Girolamo, 2025: Errors in stereoscopic retrievals of cloud top height for single-layer clouds. Atmospheric Measurement Techniques, 18, 3009–3033, https://doi.org/10.5194/amt-18-3009-2025.

Loveridge, J., A. Levis, L. Di Girolamo, V. Holodovsky, L. Forster, A. B. Davis, and Y. Y. Schechner, 2023a: Retrieving 3D distributions of atmospheric particles using Atmospheric Tomography with 3D Radiative Transfer – Part 1: Model description and Jacobian calculation. Atmospheric Measurement Techniques, 16, 1803–1847, https://doi.org/10.5194/amt-16-1803-2023.

Loveridge, J., A. Levis, L. Di Girolamo, V. Holodovsky, L. Forster, A. B. Davis, and Y. Y. Schechner, 2023b: Retrieving 3D distributions of atmospheric particles using Atmospheric Tomography with 3D Radiative Transfer – Part 2: Local optimization. Atmospheric Measurement Techniques, 16, 3931–3957, https://doi.org/10.5194/amt-16-3931-2023.

Luna-Niño, R., A. Gershunov, F. M. Ralph, A. Weyant, K. Guirguis, M. J. DeFlorio, D. R. Cayan, and A. P. Williams, 2025: Heresy in ENSO teleconnections: atmospheric rivers as disruptors of canonical seasonal precipitation anomalies in the Southwestern US. Clim Dyn, 63, 115, https://doi.org/10.1007/s00382-025-07583-1.

Markowski, P. M., E. N. Rasmussen, and J. M. Straka, 1998: The Occurrence of Tornadoes in Supercells Interacting with Boundaries during VORTEX-95. Weather and Forecasting, 13, 852–859, https://doi.org/10.1175/1520-0434(1998)013%253C0852:TOOTIS%253E2.0.CO;2.

Marquis, J. N., A. C. Varble, P. Robinson, T. C. Nelson, and K. Friedrich, 2021: Low-Level Mesoscale and Cloud-Scale Interactions Promoting Deep Convection Initiation. Monthly Weather Review, 149, 2473–2495, https://doi.org/10.1175/MWR-D-20-0391.1.

McGrath-Spangler, E. L., and A. S. Denning, 2013: Global seasonal variations of midday planetary boundary layer depth from CALIPSO space-borne LIDAR. Journal of Geophysical Research: Atmospheres, 118, 1226–1233, https://doi.org/10.1002/jgrd.50198.

Miglietta, M. M., and R. Rotunno, 2009: Numerical Simulations of Conditionally Unstable Flows over a Mountain Ridge. Journal of the Atmospheric Sciences, 66, 1865–1885, https://doi.org/10.1175/2009JAS2902.1.

Millán, L. F., and Coauthors, 2024: Water vapor measurements inside clouds and storms using a differential absorption radar. Atmospheric Measurement Techniques, 17, 539–559, https://doi.org/10.5194/amt-17-539-2024.

Nelson, K. J., F. Xie, C. O. Ao, and M. I. Oyola-Merced, 2021: Diurnal Variation of the Planetary Boundary Layer Height Observed from GNSS Radio Occultation and Radiosonde Soundings over the Southern Great Plains. Journal of Atmospheric and Oceanic Technology, 38, 2081–2093, https://doi.org/10.1175/JTECH-D-20-0196.1.

Nelson, K. J., C. O. Ao, F. Xie, J. Zawislak, and K.-N. Wang, 2025: Assessing the Quality of GNSS Radio Occultation Observations in Tropical Cyclones and Implications for Future Observations. Journal of Atmospheric and Oceanic Technology, 42, 793–814, https://doi.org/10.1175/JTECH-D-24-0027.1.

Nesbitt, S. W., and E. J. Zipser, 2003: The Diurnal Cycle of Rainfall and Convective Intensity according to Three Years of TRMM Measurements. Journal of Climate, 16, 1456–1475, https://doi.org/10.1175/1520-0442(2003)016%253C1456:TDCORA%253E2.0.CO;2.

Olson, J. B., and Coauthors, 2019: Improving Wind Energy Forecasting through Numerical Weather Prediction Model Development. Bulletin of the American Meteorological Society, 100, 2201–2220, https://doi.org/10.1175/BAMS-D-18-0040.1.

Ouyed, A., N. Smith, X. Zeng, T. Galarneau Jr., H. Su, and R. D. Dixon, 2023: Global Three-Dimensional Water Vapor Feature-Tracking for Horizontal Winds Using Hyperspectral Infrared Sounder Data From Overlapped Tracks of Two Satellites. Geophysical Research Letters, 50, e2022GL101830, https://doi.org/10.1029/2022GL101830.

Padullés, R., E. Cardellach, M. de la Torre Juárez, S. Tomás, F. J. Turk, S. Oliveras, C. O. Ao, and A. Rius, 2016: Atmospheric polarimetric effects on GNSS radio occultations: the ROHP-PAZ field campaign. Atmospheric Chemistry and Physics, 16, 635–649, https://doi.org/10.5194/acp-16-635-2016.

Palm, S. P., P. Selmer, J. Yorks, S. Nicholls, and E. Nowottnick, 2021: Planetary Boundary Layer Height Estimates From ICESat-2 and CATS Backscatter Measurements. Front. Remote Sens., 2, https://doi.org/10.3389/frsen.2021.716951.

Pan, Y., S. Zhang, Q. Li, L. Ma, S. Jiang, L. Lei, W. Lyu, and Z. Wang, 2020: Analysis of convective instability data derived from a ground-based microwave radiometer before triggering operations for artificial lightning. Atmospheric Research, 243, 105005, https://doi.org/10.1016/j.atmosres.2020.105005.

Parker, M. D., 2008: Response of Simulated Squall Lines to Low-Level Cooling. Journal of the Atmospheric Sciences, 65, 1323–1341, https://doi.org/10.1175/2007JAS2507.1.

Paz, A., R. Padullés, and E. Cardellach, 2024: Evaluating the Polarimetric Radio Occultation Technique Using NEXRAD Weather Radars. Remote Sensing, 16, 1118, https://doi.org/10.3390/rs16071118.

Rabinowitz, J. L., A. R. Lupo, P. S. Market, and P. E. Guinan, 2019: An investigation of atmospheric rivers impacting heavy rainfall events in the North-Central Mississippi River Valley. International Journal of Climatology, 39, 4091–4106, https://doi.org/10.1002/joc.6061.

Rahimi, B., and U. Foelsche, 2025: The potential of observing atmospheric rivers with Global Navigation Satellite System (GNSS) radio occultation. Atmospheric Measurement Techniques, 18, 2481–2507, https://doi.org/10.5194/amt-18-2481-2025.

Rappin, E. D., and D. S. Nolan, 2012: The effect of vertical shear orientation on tropical cyclogenesis. Quarterly Journal of the Royal Meteorological Society, 138, 1035–1054, https://doi.org/10.1002/qj.977.

Reinking, R. F., R. J. Doviak, and R. O. Gilmer, 1981: Clear-Air Roll Vortices and Turbulent Motions as Detected with an Airborne Gust Probe and Dual-Doppler Radar. Journal of Applied Meteorology and Climatology, 20, 678–685, https://doi.org/10.1175/1520-0450(1981)020%253C0678:CARVAT%253E2.0.CO;2.

Ruane, A. C., and Coauthors, 2022: The Climatic Impact-Driver Framework for Assessment of Risk-Relevant Climate Information. Earth's Future, 10, e2022EF002803, https://doi.org/10.1029/2022EF002803.

Schumacher, C., and A. Funk, 2023: Assessing Convective-Stratiform Precipitation Regimes in the Tropics and Extratropics With the GPM Satellite Radar. Geophysical Research Letters, 50, e2023GL102786, https://doi.org/10.1029/2023GL102786.

Shrestha, B., J. A. Brotzge, J. Wang, N. Bain, C. D. Thorncroft, E. Joseph, J. Freedman, and S. Perez, 2021: Overview and Applications of the New York State Mesonet Profiler Network. Journal of Applied Meteorology and Climatology, 60, 1591–1611, https://doi.org/10.1175/JAMC-D-21-0104.1.

Tang, B., and K. Emanuel, 2012: A Ventilation Index for Tropical Cyclones. Bulletin of the American Meteorological Society, 93, 1901–1912, https://doi.org/10.1175/BAMS-D-11-00165.1.

Teixeira, J., and Coauthors, 2025: Toward a Global Planetary Boundary Layer Observing System: A Summary. Bulletin of the American Meteorological Society, 106, E1566–E1579, https://doi.org/10.1175/BAMS-D-23-0228.1.

Tornow, F., A. S. Ackerman, A. M. Fridlind, G. Tselioudis, B. Cairns, D. Painemal, and G. Elsaesser, 2023: On the Impact of a Dry Intrusion Driving Cloud-Regime Transitions in a Midlatitude Cold-Air Outbreak. Journal of the Atmospheric Sciences, 80, 2881–2896, https://doi.org/10.1175/JAS-D-23-0040.1.

Turner, D. D., and U. Löhnert, 2021: Ground-based temperature and humidity profiling: combining active and passive remote sensors. Atmospheric Measurement Techniques, 14, 3033–3048, https://doi.org/10.5194/amt-14-3033-2021.

Vergados, P., A. J. Mannucci, and H. Su, 2013: A validation study for GPS radio occultation data with moist thermodynamic structure of tropical cyclones. Journal of Geophysical Research: Atmospheres, 118, 9401–9413, https://doi.org/10.1002/jgrd.50698.

Viscardi, L. A. M., G. Torri, D. K. Adams, and H. de M. J. Barbosa, 2024: Environmental controls on isolated convection during the Amazonian wet season. Atmospheric Chemistry and Physics, 24, 8529–8548, https://doi.org/10.5194/acp-24-8529-2024.

——, ——, ——, and ——, 2025: Sensitivity of the Shallow-To-Deep Convective Transition to Moisture and Wind Shear in the Amazon. Journal of Advances in Modeling Earth Systems, 17, e2024MS004238, https://doi.org/10.1029/2024MS004238.

——, J. L. Garrison, U. Acikoz, J. S. Haase, B. J. Murphy, P. Muradyan, and T. Lulich, 2016: Open-Loop Tracking of Rising and Setting GPS Radio-Occultation Signals From an Airborne Platform: Signal Model and Error Analysis.

IEEE Transactions on Geoscience and Remote Sensing, 54, 3967–3984, https://doi.org/10.1109/TGRS.2016.2532346.

Weckwerth, T. M., 2000: The Effect of Small-Scale Moisture Variability on Thunderstorm Initiation. Monthly Weather Review, 128, 4017–4030, https://doi.org/10.1175/1520-0493(2000)129%253C4017:TEOSSM%253E2.0.CO;2.

——, J. W. Wilson, and R. M. Wakimoto, 1996: Thermodynamic Variability within the Convective Boundary Layer Due to Horizontal Convective Rolls. Monthly Weather Review, 124, 769–784, https://doi.org/10.1175/1520-0493(1996)124%253C0769:TVWTCB%253E2.0.CO;2.

Wu, F., and K. Lombardo, 2021: Precipitation Enhancement in Squall Lines Moving over Mountainous Coastal Regions. Journal of the Atmospheric Sciences, 78, 3089–3113, https://doi.org/10.1175/JAS-D-20-0222.1.

——, and ——, 2023: The Impact of Offshore‐Propagating Squall Lines on Coastal‐Mountain Flows. Geophysical Research Letters, 50, e2023GL102825, https://doi.org/10.1029/2023GL102825.

Wulfmeyer, V., and Coauthors, 2021: Exploring Terra Incognita in the Earth System: The GEWEX Land-Atmosphere Feedback Observatory (GLAFO). GEWEX [White Paper].

Yang, G.-Y., and J. Slingo, 2001: The Diurnal Cycle in the Tropics. Monthly Weather Review, 129, 784–801, https://doi.org/10.1175/1520-0493(2001)129%253C0784:TDCITT%253E2.0.CO;2.

Yu, C.-L., A. C. Didlake, and F. Zhang, 2022: Updraft Maintenance and Axisymmetrization during Secondary Eyewall Formation in a Model Simulation of Hurricane Matthew (2016). Journal of the Atmospheric Sciences, 79, 1105–1125, https://doi.org/10.1175/JAS-D-21-0103.1.

Zeng, X., and Coauthors, 2020: Use of Observing System Simulation Experiments in the United States. Bulletin of the American Meteorological Society, 101, E1427–E1438, https://doi.org/10.1175/BAMS-D-19-0155.1.

——, and Coauthors, 2024: Vientos—A New Satellite Mission Concept for 3D Wind Measurements by Combining Passive Water Vapor Sounders with Doppler Wind Lidar. Bulletin of the American Meteorological Society, 105, E357–E369, https://doi.org/10.1175/BAMS-D-22-0283.1.

——, and Coauthors, 2025: Global Precipitation Experiment—A New World Climate Research Programme Lighthouse Activity. Bulletin of the American Meteorological Society, 106, E408–E418, https://doi.org/10.1175/BAMS-D-23-0242.1.

Zhang, J. A., R. F. Rogers, P. D. Reasor, E. W. Uhlhorn, and F. D. Marks, 2013: Asymmetric Hurricane Boundary Layer Structure from Dropsonde Composites in Relation to the Environmental Vertical Wind Shear. Monthly Weather Review, 141, 3968–3984, https://doi.org/10.1175/MWR-D-12-00335.1.

Zhang, Y. D. J. Stensrud, C. Lyn Comer, and B. Stouffer, 2025: Assimilating Novel Boundary Layer Observations from Dual-Polarization Radars to Improve Lower-Tropospheric Moisture and Torrential Rainfall Forecasts. Monthly Weather Review, 309-326, https://doi.org/10.1175/MWR-D-24-0154.1.

Zhao, G., and L. Di Girolamo, 2007: Statistics on the macrophysical properties of trade wind cumuli over the tropical western Atlantic. Journal of Geophysical Research: Atmospheres, 112, https://doi.org/10.1029/2006JD007371.

Ziegler, C. L., E. R. Mansell, J. M. Straka, D. R. MacGorman, and D. W. Burgess, 2010: The Impact of Spatial Variations of Low-Level Stability on the Life Cycle of a Simulated Supercell Storm. Monthly Weather Review, 138, 1738–1766, https://doi.org/10.1175/2009MWR3010.1.